Geomechanics and Engineering, *Vol. 35, No. 1 (2023) 55-65*
https://doi.org/10.12989/gae.2023.35.1.055

Modelling creep behavior of soft clay by incorporating updated volumetric and deviatoric strain-time equations

Chen Ge[1a], Zhu Jungao[1b], Li Jian[2,4c], Wu Gang[3,4d] and Guo Wanli*[5]

[1]*Key Laboratory of Ministry of Education for Geomechanics and Embankment Engineering, Hohai University, Nanjing 210098, China*
[2]*Chengdu Engineering Corporation Limited, Chengdu 610072, China*
[3]*Huaneng Tibet Yarlungzangbo River Hydropower Development and Investment Co. Ltd, Beijingxi Road, Tibet 850000, China*
[4]*Huaneng Tibet Hydropower Safety Engineering Technology Research Center, Beijingxi Road, Tibet 850000, China*
[5]*Geotechnical Engineering Department, Nanjing Hydraulic Research Institute, Nanjing 210024, China*

(*Received February 23, 2023, Revised August 23, 2023, Accepted August 28, 2023*)

Abstract. Soft clay is widely spread in nature and encountered in geotechnical engineering applications. The creep property of soft clay greatly affects the long-term performance of its upper structures. Therefore, it is vital to establish a reasonable and practical creep constitutive model. In the study, two updated hyperbolic equations based on the volumetric creep and deviatoric creep are respectively proposed. Subsequently, three creep constitutive models based on different creep behavior, i.e., V-model (use volumetric creep equation), D-model (use deviatoric creep equation) and VD-model (use both volumetric and deviatoric creep equations) are developed and compared. From the aspect of prediction accuracy, both V-model and D-model show good agreements with experimental results, while the predictions of the VD-model are smaller than the experimental results. In terms of the parametric sensitivity, D-model and VD-model are lower sensitive to parameter M (the slope of the critical state line) than V-model. Therefore, the D-model which is developed by incorporating the updated deviatoric creep equation is suggested in engineering applications.

Keywords: creep constitutive model; deviator creep; hyperbolic equation; soft clay; volumetric creep

1. Introduction

The top layers of soil in the southeastern part of China predominantly consist of soft clay. This area is densely populated, implying many building activities in and on these soft clay layers. However, soft clay exhibits pronounced creep deformation under constant stress, which poses a challenge for the secure and cost-effective design of buildings. For instance, settlement and lateral displacement of the soft clay ground embankment, as well as the lateral deformation of soft clay slopes, have been proven to be related to creep (Hessam and Mohammad 2012, Thu *et al*. 2015, Ramadhika *et al*. 2018, Li *et al*. 2019, Zhu *et al*. 2019, Long *et al*. 2020, Bi *et al*. 2022). It is well-accepted that a proper creep constitutive model is fundamental to predict the creep deformation of soft clay accurately.

In recent years, various creep constitutive models have been proposed (Yao *et al*. 2015, Rezania *et al*. 2016, Chen *et al*. 2021, Yin *et al*. 2023), the most famous among which is the Singh-Mitchell model (Singh and Mitchell 1968). The Singh-Mitchell model associates the soft clay model to a deviatoric creep behavior. This model represents stress-strain and strain-time relationships through an exponential function and a power function, respectively. The main advantages of this model lie in its parameters possessing clear physical significance and their ease of acquisition through triaxial creep tests. However, the model is valid only for $0.3<D_r<0.9$ (Borja and Kavazanjian 1985) or $0.2<D_r<0.9$ (Acharya *et al*. 2018). Moreover, Zhu *et al*. (2006) improved the Singh-Mitchell creep model of soft clays based on Mesri model and a series of laboratory triaxial creep tests conducted on soft clays from the Pearl River Delta, and It was discovered that the values of the improved Singh-Mitchell creep model parameters vary with drained conditions. Thus, it is imperative for the proposed model to account for drained conditions.

In addition, the volumetric creep behavior of soft clay has also been widely integrated into creep constitutive models, such as Taylor's secondary consolidation creep model (Taylor 1948) and Yin's EVP model (Yin and Graham 1989, 1994). The initially-proposed classical EVP model encompasses only two parameters, i.e., ψ/V and t_0, both of which are derived from creep tests. However, as time t increases, the strain tends to increases infinitely, which means that there is no upper limit of creep. To address this limitation, a novel nonlinear logarithmic function was proposed (Yin 1999, Chen *et al*. 2021), which is essentially a hyperbolic function. The model's predictions show a good fit with the experimental results.

Simultaneously, there exist certain constitutive models that link the creep model to both volumetric and deviatoric

*Corresponding author, Ph.D.
E-mail: wlguo@nhri.cn
[a]Ph.D.
E-mail: gechenhhu@163.com
[b]Professor
[c]Ph.D.
[d]Ph.D.

ISSN: 2005-307X (Print), 2092-6219 (Online)

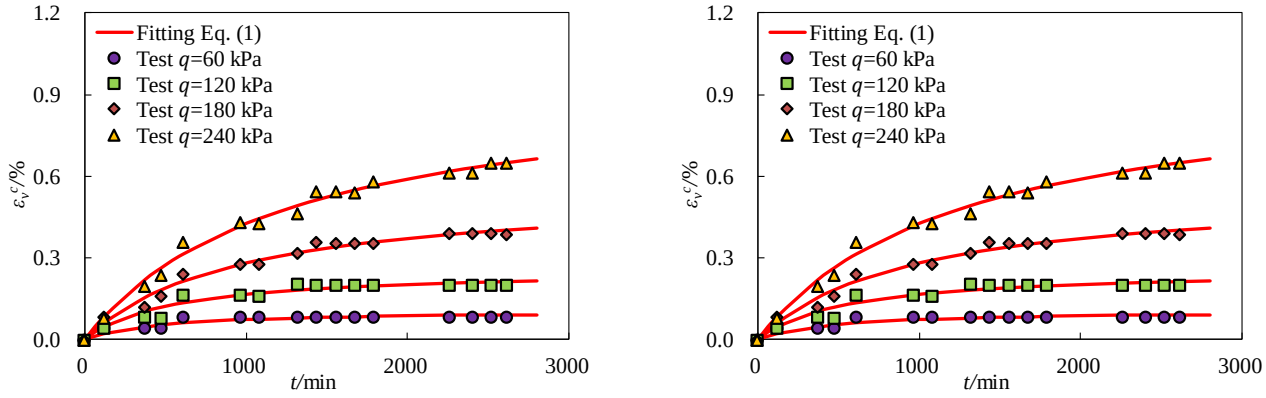

(a) σ_3=150 kPa (b) σ_3=200 kPa

Fig. 1 Evolution of volumetric creep strain with time for Cangzhou reconstituted clay under different deviatoric stresses q and confining pressures σ_3 (Liu 2020)

creep behavior. (Kavvadas and Kalos 2019, Venda Oliveira *et al*. 2019). Borja and Kavazanjian (1985) suggested that deviatoric creep strain and volumetric creep strain are estimated using Singh-Mitchell's creep law and Taylor's secondary consolidation creep law (Taylor 1948), respectively. The flow surface is assumed to have the same form as the elliptic yield surface of the Modified Cam-Clay based models (Hsieh *et al*. 1990, Borja 1992, Morsy *et al*. 1995). Oliveira *et al*. (2019) analyzed the predictive capability of Borja's model in estimating the creep behavior of soft clay under preloading conditions. The numerical results show that the impact of deviatoric creep for the long-term behavior on clay behavior is negligible compared to the effect of volumetric creep. Liu (2008) associated the volumetric and deviatoric creep laws (described by Taylor's and Mesri shear creep laws (Mesri *et al*. 1981)) to the Prandtl-Reuss flow rule (Jiang and Mu 1984).

In summary, various constitutive models are established based on volumetric creep behavior, deviatoric creep behavior, or a combined consideration of both in soft clay. So far, there is limited research that explores the distinctions among these three types of creep constitutive models. Thus, this paper introduces two refined hyperbolic equations for the relationship between strain and time, grounded in volumetric creep and deviatoric creep behaviors. These equations are verified by a comprehensive collection of laboratory test results. The three constitutive models were derived by considering different creep behavior. Further, a comparative analysis was carried out on the three models.

2. Empirical equations of creep strain with time

2.1 An updated hyperbolic equation of volumetric creep strain with time

Referring to the experimental results of various studies (Chen *et al*. 2003, Hu 2013, Liu 2020), the volumetric creep values of soft clays under different stress states has been obtained, such as Fig. 1.

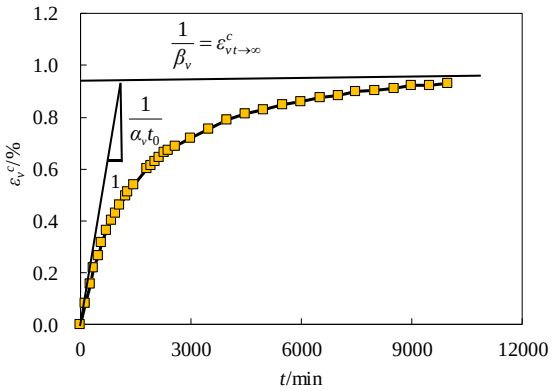

Fig. 2 Schematic diagram of the physical meaning of α_v and β_v

A hyperbolic equation describing the relationship between volumetric creep strain and time can be obtained as Eq. (1) by fitting the data points in Fig. 1.

$$\varepsilon_v^c = \frac{t}{\alpha_v t_0 + \beta_v t} \tag{1}$$

where ε_v^c is the volumetric strain of soft clay after the creep starting for a period of time t. The parameter t_0 =1440min (equivalent to one day) is used to render the equation dimensionless. α_v and β_v are two soil mechanical parameters related to stress state. $\alpha_v t_0$ equals to the reciprocal of the limiting volumetric creep strain. Parameter β_v equals to the reciprocal of the initial volumetric creep strain rate. A schematic diagram is presented in Fig. 2.

It has been observed that parameters α_v and β_v exhibit variations corresponding to different confining pressures and deviatoric stress states. α_v is related to the effective deviatoric stress q and β_v is related to the effective stress ratio q/p. The computed results of two parameters are plotted in the plane of α_v-q/p_a and β_v-q/p, respectively, in Figs. 3 and 4. The standard atmospheric pressure p_a is used for dimensionless transformation, p_a=100 kPa. Notably, the figures demonstrate that the empirical relationships Eqs. (2) and (3) effectively describe the fitted test points.

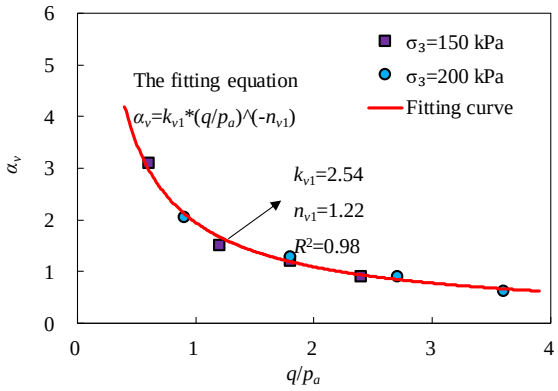

Fig. 3 Relationship between α_v and q/p_a for Cangzhou reconstituted clay

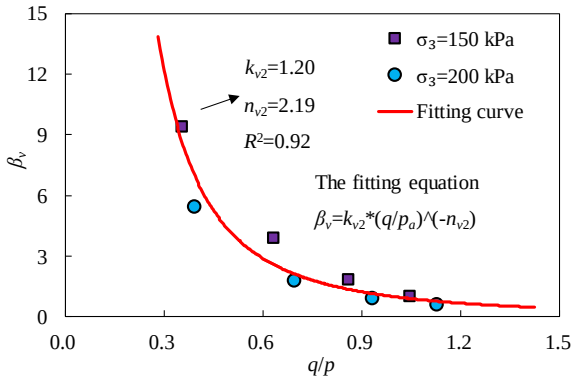

Fig. 4 Relationship between β_v and q/p for Cangzhou reconstituted clay

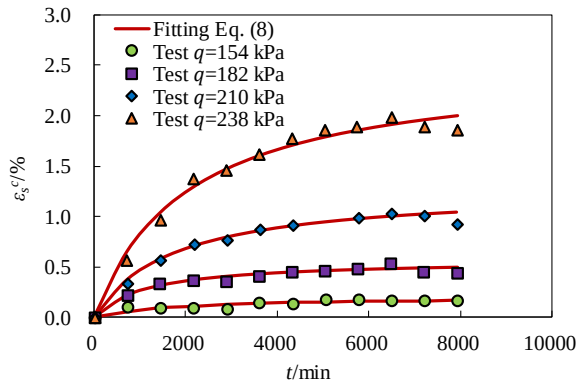

(a) Zhuhai clay (Hu 2013)

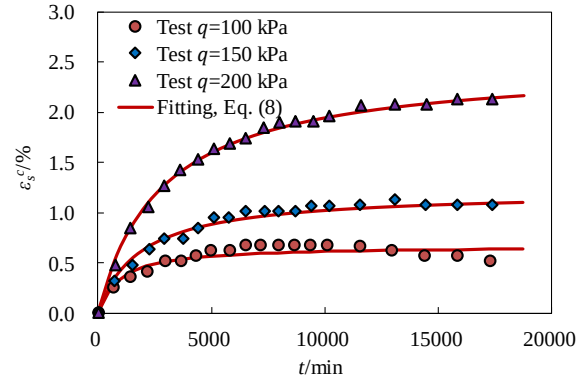

(b) Shantou to Jieyang high-speed road soft clay (Dong 2007)

Fig. 5 Measured and calculated deviatoric strain with time of clay under confining pressure of 100 kPa

$$\alpha_v = k_{v1}(\frac{q}{p_a})^{-n_{v1}} \tag{2}$$

$$\beta_v = k_{v2}(\frac{q}{p})^{-n_{v2}} \tag{3}$$

where k_{v1}, n_{v1}, k_{v2} and n_{v2} are non-dimensional soil mechanical parameters. q is the effective deviatoric stress. p is the effective mean normal stress. In triaxial tests, $q=\sigma_1-\sigma_3$, $p=(\sigma_1+2\sigma_3)/3$.

From the expressions for α_v and β_v (given Eqs. (2) and (3)), Eq. (1) can be rewritten as Eq. (4), which is the final expression of volumetric creep strain under general stress state.

$$\varepsilon_v^c = \frac{t}{k_{v1}(\frac{q}{p_a})^{-n_{v1}}t_0 + k_{v2}(\frac{q}{p})^{-n_{v2}}t} \tag{4}$$

2.2 An updated hyperbolic equation of deviatoric creep strain with time

Based on the results of a large number of drained triaxial creep tests, the variation trend of strain-time curve is analyzed in (Chen *et al*. 2003, Dong 2007, Hu 2013, Liu 2020). It is found that evolution of deviatoric creep strain with time is similar to that of volumetric creep strain with time. A hyperbolic deviatoric creep Eq. (5) is therefore proposed as follows.

$$\varepsilon_s^c = \frac{t}{\alpha_s t_0 + \beta_s t} \tag{5}$$

where ε_s^c is the deviatoric strain of soft clay after the creep starting for a period of time t. α_s and β_s represent two soil mechanical parameters, which can be acquired through drained triaxial creep tests. Based on Eq. (5), the parameter α_s is related to the initial deviatoric creep strain rate. $\alpha_s t_0$ equals to the reciprocal of the initial slope of ε_s^c-t curve (i.e., the initial deviatoric creep strain rate). The parameter β_s equals to the reciprocal of the limiting deviatoric creep strain.

Similar to volumetric creep model parameters, α_s and β_s are assumed as Eqs. (6) and (7), respectively.

$$\alpha_s = k_{s1}(\frac{q}{p_a})^{-n_{s1}} \tag{6}$$

$$\beta_s = k_{s2}(\frac{q}{p})^{-n_{s2}} \tag{7}$$

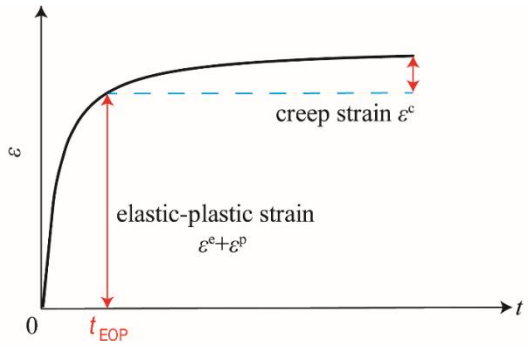

(a) Curve of ε-t

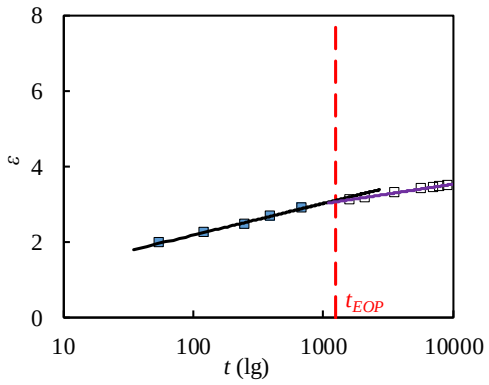

(b) Curve of ε-lg$t$

Fig. 6 Schematic diagram of strain with time for creep of soft clays (It assumes that creep occurs at the end of primary consolidation)

where k_{s1}, n_{s1}, k_{s2} and n_{s2} are non-dimensional soil mechanical parameters.

Substituting Eqs. (6) and (7) into Eq. (5) results in Eq. (8), which is the final expression of deviatoric creep strain under general stress state.

$$\varepsilon_s^c = \frac{t}{k_{s1}(\frac{q}{p_a})^{-n_{s1}} t_0 + k_{s2}(\frac{q}{p})^{-n_{s2}} t} \tag{8}$$

Clays of Zhuhai (Hu 2013) and the foundation of the Shantou to Jieyang high-speed railway in China (Dong 2007) were employed to validate the accuracy of Eq. (8).

The predicted results of different deviatoric stress levels using the obtained parameters from Eq. (8) and the test data are shown in Fig. 5. It is observed that the curves of the proposed equation agree well with the test data under different stress states, indicating that Eq. (8) is able to describe the deviatoric creep strain of soft clays.

3. Three models incorporating different creep behaviour

3.1 Creep strain component

It is assumed that the whole deformation process of soft clay is divided into elastic-plastic deformation unrelated to time and creep deformation related to time, and can be written as Eq. (9).

$$\varepsilon = \begin{cases} \varepsilon^e + \varepsilon^p, t \le t_{EOP} \\ \varepsilon^e + \varepsilon^p + \varepsilon^c, t > t_{EOP} \end{cases} \tag{9}$$

where ε is the total strain. ε^e is the elastic strain. ε^c is the creep strain. ε^p is the plastic strain. t is the time of deformation. t_{EOP} is the ending time of primary consolidation. The ending time of primary consolidation t_{EOP} is related to types, thickness, pressure of soils and so on. Many scholars proposed the inflection point of ε-t curve as the ending time of primary consolidation, or intersection point of two lines in the plane of ε-lg$t$ is regarded as the ending time of primary consolidation t_{EOP}. Schematic diagram of t_{EOP} is shown in Fig. 6. The elastoplastic strain ε^e and ε^p are consistent with the modified Cam-Clay (MCC) model. The volumetric creep and deviatoric creep strain of soft clay (i.e., the creep strain ε^c) are computed as described above according to the results of triaxial tests in various areas.

The creep constitutive model is commonly described in incremental form in order to adapt to the numerical implementation in the generic finite element framework. According to the characteristics of viscosity of soils, the total incremental strain $d\varepsilon_{ij}$ is the sum of an elastic incremental strain $d\varepsilon_{ij}^e$, a plastic incremental strain $d\varepsilon_{ij}^p$ and a creep incremental strain $d\varepsilon_{ij}^c$, which can be expressed by Eq. (10).

$$d\varepsilon_{ij} = d\varepsilon_{ij}^e + d\varepsilon_{ij}^p + d\varepsilon_{ij}^c \tag{10}$$

The elastic incremental strain $d\varepsilon_{ij}^e$ and plastic incremental strain $d\varepsilon_{ij}^p$ are expressed respectively by Eqs. (23) and (24) in Appendix A. The calculation processes of creep incremental strain $d\varepsilon_{ij}^c$ will be introduced in next sections.

3.2 V-model using volumetric creep equation

There is a plastic potential surface in the study of plastic strain. Similarly, there is a flow surface Q in the study of creep deformation. Based on the flow rule proposed by Perzyna (1966), Yin (1999) suggested that the components of creep strain are described as Eq. (11).

$$\frac{d\varepsilon_{ij}^c}{dt} = dS\frac{\partial Q}{\partial \sigma_{ij}} \tag{11}$$

where Q is the creep strain rate flow surface function. dS is the creep scaling function, which determines the magnitude of the creep strain.

It is assumed that the Q in Eq. (11) has the same form as the elliptic yield surface function of the MCC model, that is, $Q=f$. The volumetric creep behavior of soft clay is adopted to creep constitutive model. Thus, Eq. (11) becomes Eq. (12).

$$\frac{d\varepsilon_v^c}{dt} = dS\frac{\partial Q}{\partial p} = dS\frac{\lambda-\kappa}{1+e_0}\frac{1}{p}\frac{M^2p^2-q^2}{M^2p^2+q^2} \tag{12}$$

By differentiating Eq. (4) with respect to t, volumetric creep stain rate is described by Eq. (13).

$$\frac{d\varepsilon_v^c}{dt}=\frac{k_{v1}(\frac{q}{p_a})^{-n_{v1}}t_0}{\left[k_{v1}(\frac{q}{p_a})^{-n_{v1}}t_0+k_{v2}(\frac{q}{p})^{-n_{v2}}t\right]^2} \tag{13}$$

t is described by Eq. (14) according to Eq. (4)

$$t=\frac{\varepsilon_v^c k_{v1}(\frac{q}{p_a})^{-n_{v1}}}{1-\varepsilon_v^c k_{v2}(\frac{q}{p})^{-n_{v2}}}t_0 \tag{14}$$

From Eq. (14) and Eq. (13), the final volumetric creep stain rate is described as Eq. (15).

$$\frac{d\varepsilon_v^c}{dt}=\frac{\left[1-\varepsilon_v^c k_{v2}(\frac{q}{p})^{-n_{v2}}\right]^2}{\left[k_{v1}(\frac{q}{p_a})^{-n_{v1}}t_0\right]} \tag{15}$$

The creep scaling function is expressed as Eq. (16) by combining Eqs. (12) and (15).

$$dS=\frac{\left[1-\varepsilon_v^c k_{v2}(\frac{q}{p})^{-n_{v2}}\right]^2}{\left[k_{v1}(\frac{q}{p_a})^{-n_{v1}}t_0\right]}\frac{(1+e_0)}{(\lambda-\kappa)}\frac{\left(M^2p^2+q^2\right)}{\left(M^2p^2-q^2\right)}p \tag{16}$$

From Eq. (16) and Eq. (11), the final creep increment under general stress state can be obtained as Eq. (17). The final creep constitutive model V-model which is developed by incorporating the updated volumetric creep equation is obtained hence (Eq. (25) in the Appendix B).

$$d\varepsilon_{ij}^c=dS\frac{dg}{d\sigma_{ij}}dt=dS\left(\frac{\partial g}{\partial p}\frac{\partial p}{\partial \sigma_{ij}}+\frac{\partial g}{\partial q}\frac{\partial q}{\partial \sigma_{ij}}\right)dt=\left[\frac{\delta_{ij}}{3}+\frac{3p(\sigma_{ij}-p\delta_{ij})}{M^2p^2-q^2}\right]\frac{\left[1-\varepsilon_v^c k_{v2}(q/p)^{-n_{v2}}\right]^2}{\left[k_{v1}(q/p_a)^{-n_{v1}}t_0\right]}dt \tag{17}$$

As described above, t_0=1440min, the initial void ratio e_0 can be obtained from survey data. Thus, there are actually eight parameters in V-model. Parameters M, λ, κ and μ are related to elastic-plastic deformation. Parameters M is the slope of the critical state line. It is easily obtained from laboratory conventional triaxial test data. λ and κ are measured from conventional 1-day loading oedometer test results. The value of Poisson's ratio μ for each clay is selected according to previous experience. Parameters k_{v1}, k_{v2}, n_{v1} and n_{v2}, related to volumetric creep deformation, are obtained by laboratory triaxial creep test, as noted previously.

3.3 D-model using deviatoric creep equation

Similar to the derivation process of section 3.2, the flow proportional equation of deviatoric creep component can be got from empirical Eq. (8) as follows

$$\frac{d\varepsilon_s^c}{dt}=dS\frac{\partial Q}{\partial q}=dS\frac{\lambda-\kappa}{1+e_0}\frac{2q}{M^2p^2+q^2} \tag{18}$$

Then, the final creep increment of D-model under general stress state can be obtained as Eq. (19).

$$d\varepsilon_{ij}^c=dS\left(\frac{\partial g}{\partial p}\frac{\partial p}{\partial \sigma_{ij}}+\frac{\partial g}{\partial q}\frac{\partial q}{\partial \sigma_{ij}}\right)dt=\left[\frac{M^2p^2-q^2}{M^2p^2+q^2}\frac{\delta_{ij}}{3p}+\frac{3(\sigma_{ij}-p\delta_{ij})}{2q}\right]\frac{\left[1-\varepsilon_s^c k_{s2}(q/p)^{-n_{s2}}\right]^2}{\left[k_{s1}(q/p_a)^{-n_{s1}}t_0\right]}dt \tag{19}$$

The final creep constitutive model D-model considering the deviatoric creep behavior is built (Eq. (26) in the Appendix C). As described above, there are eight parameters in D-model. Parameters M, λ, κ and μ are related to elastic-plastic deformation. The physical meanings of the four parameters have been explained in the previous section. Parameters k_{s1}, k_{s2}, n_{s1} and n_{s2}, related to deviatoric creep deformation, are obtained by laboratory triaxial creep tests.

3.4 VD-model using both volumetric and deviatoric creep equations

VD-model associates the soft clay model to the volumetric and deviatoric creep. According to Prandtl-Reuss flow rule (Jiang and Mu 1984) that assumes the Q has the same form as the Mises yield function (von Mises 1913), strain increment is expressed as Eq. (20).

$$\varepsilon_{ij}=\frac{I}{3}\varepsilon_v+\varepsilon_s\frac{s_{ij}}{q} \tag{20}$$

where $I=\begin{bmatrix}1 & 1 & 1 & 0 & 0 & 0\end{bmatrix}^T$, s_{ij} is deviator strain tensor,

$$s_{ij}=\begin{bmatrix}s_x & s_y & s_z & 2\tau_{xy} & 2\tau_{yz} & 2\tau_{zx}\end{bmatrix}^T$$

According to Eq. (20), the final creep increment of VD-model can be expressed as Eq. (21).

$$d\varepsilon_{ij}^c=\left(\frac{I}{3}\frac{d\varepsilon_v^c}{dt}+\frac{d\varepsilon_s^c}{dt}\frac{s_{ij}}{q}\right)dt \tag{21}$$

Final creep constitutive model VD-model based on Prandtl-Reuss flow rule is shown in Appendix D. There are 12 parameters in the constitutive model VD-model. As above mentioned, parameters M, λ, κ and μ, related to elastic-plastic deformation, are obtained by laboratory conventional triaxial test and compression test data. Parameters k_{v1}, k_{v2}, n_{v1}, n_{v2}, k_{s1}, k_{s2}, n_{s1} and n_{s2}, related to creep deformation, are obtained by laboratory triaxial creep test.

4. Experimental validation and comparisons of three models

4.1 Prediction accuracy of three models

The equation of elastic-plastic strain for soft clays has undergone validation within pertinent literature (Roscoe and Burland 1968). Therefore, this study aims to verify and compare creep strain increments of three different models. The drainage triaxial creep tests were performed on reconstituted clay from Zhuhai to verify and compare the proposed creep models. Main physico-mechanical

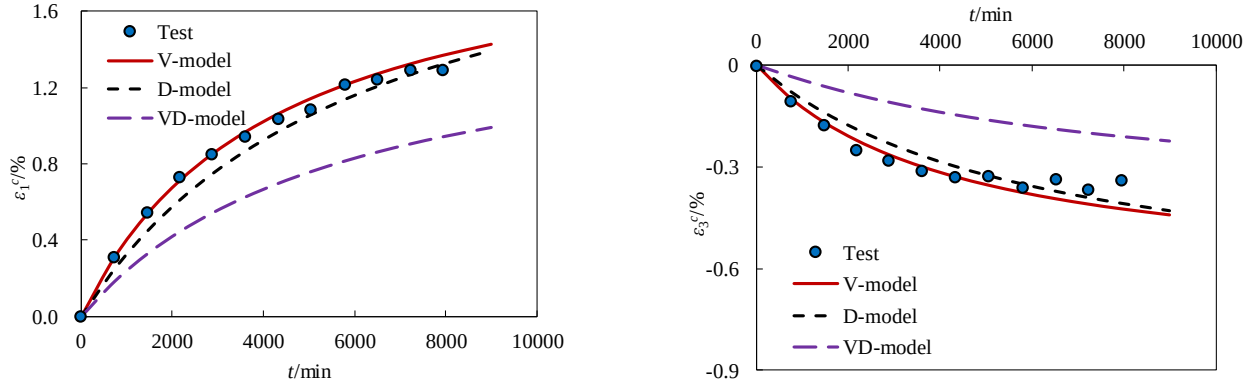

(a) major principal strain (b) minor principal strain

Fig. 7 Evolution of volumetric creep strain with time for Cangzhou reconstituted clay under different deviatoric stresses q and confining pressures σ_3 (Liu 2020)

Table 1 Main physico-mechanical properties of Zhuhai reconstituted clay (Hu 2013)

γ /(kN/m^3)	w /%	e /%	w_l /%	w_p /%
61.8	1.67	60	27	2.67

Table 2 Creep test program of soft clay from Zhuhai (Hu 2013)

σ_3 (kPa)	q (kPa)				
200	264	312	360	408	Model validation
300	357.5	422.5	487.5	552.5	Parameter solution

properties of Zhuhai clay are listed in Table 1. The details of the creep test program are presented in Table 2. The data at confining pressure of 300 kPa is employed to determine the model parameters, and then the test data at confining pressure of 200 kPa are utilized to assess the predictive accuracy of the three models.

The creep model parameters of Zhuhai reconstituted clay are determined using methods mentioned above (M=1.501, k_{v1}=26.47, n_{v1}=1.55, k_{v2}=2.04, n_{v2}=4.18, k_{s1}=535.22, n_{s1}=4.33, k_{s2}=1.21 and n_{s2}=7.73). The predictive values of major principal strain and minor principal strain under a confining pressure of 200 kPa are calculated by the obtained parameters and the creep increment equations (in the Appendix E). The predictions and the test data are presented in Fig. 7. The test data of q=360 kPa are taken the examples.

It is seen from Fig. 7 that the predicted trends of the three constitutive models are in basic agreement with the test data. The forecasting ability of VD-model is the poorest, and the predictions by the model are smaller than the experimental values. The predicted results of V-model and D-model show good agreements with experimental results. Despite the predictions are larger than test data in later period of creep, it is safe to use the two models in engineering design.

At the same time, laboratory drained triaxial creep tests were conducted on soft clays from Daishan to verify and compare the three models. Specimens were consolidated under a confining pressure of 200 kPa. Then, different deviatoric stresses q were imposed to these specimens while keeping the confining pressure constant. All tests lasted almost 10000 minutes and the evolution of strain with time was recorded. The creep model parameters of Daishan clay are obtained (M=0.94, k_{v1}=3.71, n_{v1}=0.21, k_{v2}=1.82, n_{v2}=0.69, k_{s1}=11.6, n_{s1}=1.01, k_{s2}=1.51 and n_{s2}=0.44). The predicted results of major principal strain and minor principal strain using the obtained parameters under fixed confining pressure of 200 kPa are compared with the test data, as indicated in Fig. 8.

It is observed from Fig. 8(a) that the trend of the major principal strain is similar to that of Zhuhai clay. The predictions from D-model compared with those from V-model and VD-model are in better agreement with the experimental data. Fig. 8(b) illustrates the minor principal strain with time. Its trend is inconsistent with that of the major principal strain. The experimental values of the minor principal strain appear positive, while the predicted values of V-model and D-model are always negative. In general, the principal strains predicted by VD-model are smaller compared with the test data. The principal strains predicted by V-model are unstable, which is larger in the early period of creep and smaller in later period of creep. The principal strains predicted by D-model are the most accurate.

Further, the creep test data for clay in Guangdong, China (Chen *et al*. 2003) are analyzed in order to validate the predictive effect of three models. The parameters are obtained M=1.5, k_{v1}=0.41, n_{v1}=1.17, k_{v2}=0.22, n_{v2}=1.19, k_{s1}=0.28, n_{s1}=1.93, k_{s2}=0.25 and n_{s2}=1.93. The predicted results of the principal strain and test data under confining pressure of 100 kPa and deviatoric stress of 112 kPa are listed in Fig. 9.

It is found from the Fig. 9 that V-model and D-Model were able to capture satisfactorily the consolidation and creep behavior, and D-Model is superior to V-model. For the minor principal strain, the predictions of V-model and D-Model slightly exceed the experimental values in later period of creep. It is safe for engineering constructions so that the influence can be ignored. The principal strains

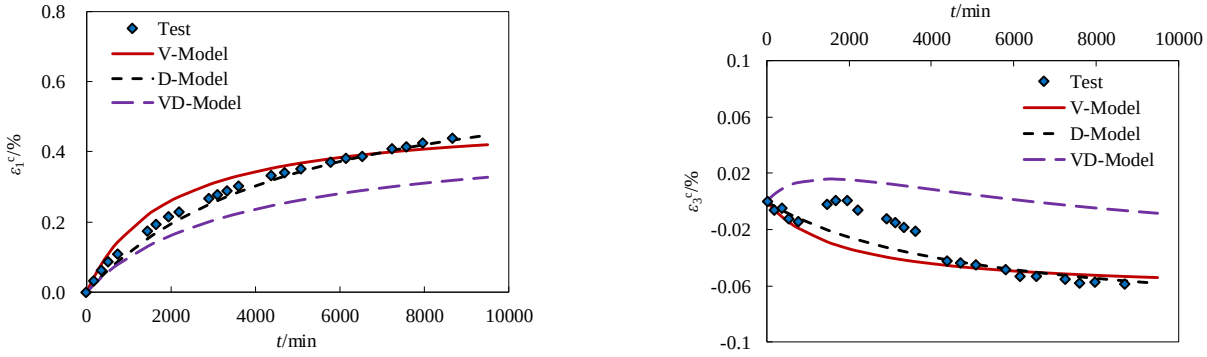

(a) major principal strain (b) minor principal strain

Fig. 8 Measured and predicted principal strain with time for Daishan clay under fixed deviatoric stress of 140 kPa and confining pressure of 200 kPa

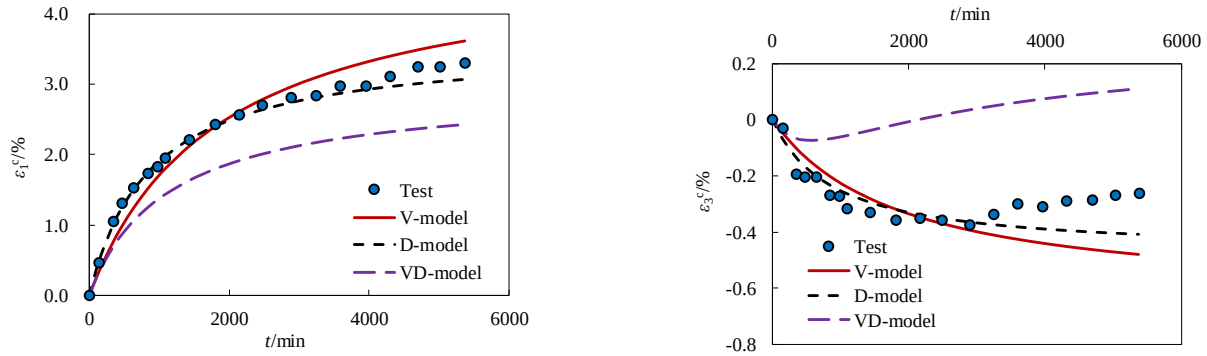

(a) major principal strain (b) minor principal strain

Fig. 9 Measured and predicted principal strain with time for Guangdong clay under fixed deviatoric stress of 112 kPa and confining pressure of 100 kPa (Chen *et al*. 2003)

predicted by VD-model are smaller than the experimental values. Therefore, VD-model clearly underpredicts the creep deformations, which is dangerous for engineering design. In addition, for the minor principal strains predicted by the VD-model, the positive values even are appeared. The results show that the predictions of D-model are the most accurate for the clay in Guangdong. It is same to Zhuhai clay and Daishan clay above.

4.2 Sensitivity analysis for three models

It is worth noting that the quality of the model depends not only on the accuracy, but also on the parametric sensitivity. The parametric sensitivity of the models may be poor even though the predictions are accurate. The model with high sensitivity leads to a larger deviation between the predictions and the test data if there are errors in the parameters, thus it is necessary to analyze further the parametric sensitivity of the models.

The parameter M determined by consolidated drained triaxial test may be larger or smaller due to the test errors. Predictions of the models will be affected if the model is highly sensitive to parameter M. It is crucial to explore the influence of parameter M on the predicted results of the models. It is found that the primary strains of VD-model are irrelevant to parameter M, i.e., VD-model is not affected by M.

Zhuhai clay is taken as an example to compare the parametric sensitivity of V-model and D-model. The sensitivity of its major principal strains to parameter M under fixed confining pressure of 200 kPa and deviatoric stress of 408 kPa is analyzed. The value of parameter M is changed under constant other parameters. M increased by 10% from 1.501 to 1.651, decreased by 10% to 1.351. Fig. 10 shows the curve of corresponding predictions with time obtained by substituting the increased or decreased M values into the two models.

Fig. 10 shows that the parametric sensitivity of D-model is lower. The predicted values of D-model for creep change slightly with the change of the parameter M. The parametric sensitivity of V-model is high, especially the predicted values increase too much as the parameter M decreases by 10%. It is indicated that V-model is inapplicable for engineering. The main reason for the high sensitivity of V-model is that the creep proportional equation dS is calibrated by volumetric creep strain in V-model. The creep strain component of V-model contains $\left(\frac{\delta_{ij}}{3}+\frac{3p(\sigma_{ij}-p\delta_{ij})}{M^2p^2-q^2}\right)$ factor, which is simplified to $\left(\frac{1}{3}+\frac{2\eta}{M^2-\eta^2}\right)$ under triaxial stress state. However, the creep proportional equation dS of D-model is calibrated by

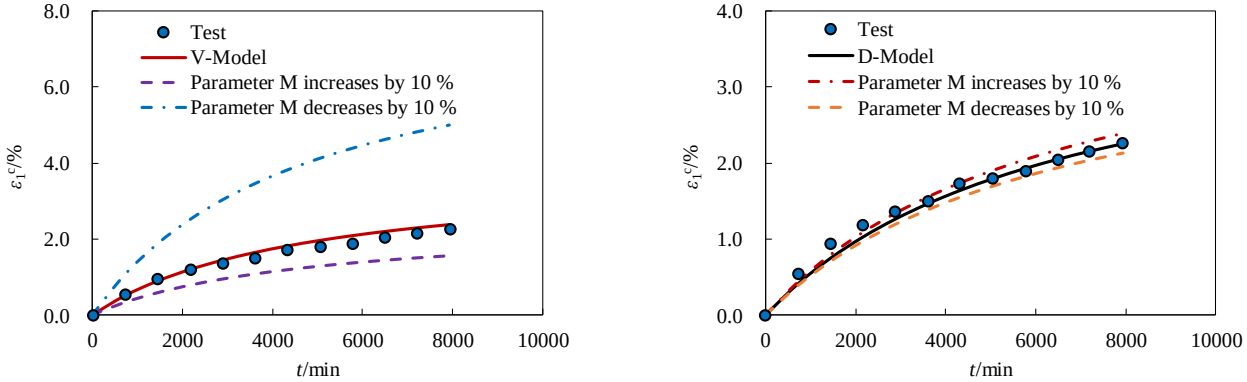

(a) V-model (b) D-model

Fig. 10 Effect of changing parameters on the predicted values of the two models

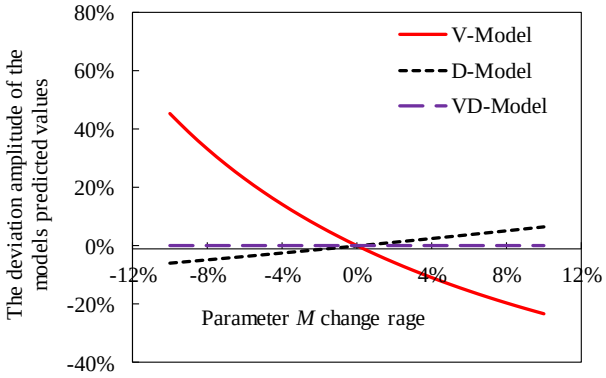

Fig. 11 Effect of the range of the parameter M on the magnitude of the model's predicted values

deviatoric creep strain. Its creep strain component contains $\left[\frac{M^2p^2-q^2}{2q}\frac{\delta_{ij}}{3p}+\frac{3(\sigma_{ij}-p\delta_{ij})}{2q}\right]$ factor, which is simplified to $\left(1+\frac{M^2-\eta^2}{6\eta}\right)$ under triaxial stress state. The factor $\left(\frac{1}{3}+\frac{2\eta}{M^2-\eta^2}\right)$ is more sensitive to the change of M than $\left(1+\frac{M^2-\eta^2}{6\eta}\right)$. Further, the variation range of the predicted values of the three models with M values from -10% to 10% are drawn in Fig. 11.

It is clearly seen from Fig. 11 that V-model is significantly affected by the parameter M. The predictions of V-model increase respectively by 18.3% and 45.2% with the parameter values decreasing by 5% and 10%, and with the parameter values increasing by 5% and 10%, the predicted values of V-model decrease by 13.3% and 23.3%, respectively. D-model is lower sensitive compared with V-model. The deviation of the predicted value of D-model is within 5% when the parameter variation range is −10%−10%.

As mentioned above, the parametric sensitivity of VD-model is the lowest, follow by D-model and the last one is V-model. Combined with the prediction accuracy of the three models, it is observed that the predicted value of VD-model is smaller than the test data resulting in VD-model is unsafe for engineering. Therefore, the applicability of D-model is the best, and it is suggested in engineering applications.

5. Discussions

In this study, three creep constitutive models are developed based on the updated hyperbolic volumetric and deviatoric creep equations. During the derivation process, we assume that elastoplastic deformation and creep deformation are clearly conducted separately. It must be acknowledged, nonetheless, that this assumption has certain flaws. For example, it fails to satisfy the developing theories in viscous behaviour of clayey soils and usually underestimates the long-term settlements (Chen *et al*, 2021). Therefore, some researchers argue that creep occurs throughout the entire consolidation process (Freitas *et al*. 2011, Zhu *et al*. 2015, Chen *et al*. 2014, Qiao *et al*. 2016, Zhao *et al*. 2018, Liu *et al*. 2019). However, most engineers primarily focus only on post-construction settlement (i.e., the creep deformation assumed in the paper) because the primary consolidation stage of soft foundations has been completed during the construction period. Therefore, it is reasonable to divide creep and primary consolidation completely in a way.

Overall, the predictions from the three models proposed in the paper agree well with the test data in different regions of China. The V-model and D-model exhibit good agreement with the laboratory test data compared to the VD-model. However, the two models show poor predictive ability for minor primary strain over time due to inherent drawbacks in the hyperbolic equation. The predictions of the updated hyperbolic equations (V-model and D-model) are monotonically increasing, whereas the test data first increase but then decrease with time. The two models cannot catch the dilative behavior for the examined soils. Moreover, it is possible that the flow surface of the MCC model may not accurately capture the creep behavior of soft clays.

Despite the fact that the VD-model underestimates creep deformations, its predicted trend is satisfactory. In other words, the VD-model (which uses both volumetric and deviatoric creep equations) seems to capture the dilative behavior of the examined soils. (e.g., data presented in Fig. 8(b) or in Fig. 9(b)). It implies that the flow surface using the Mises yield function that VD-model adopts is perhaps more reasonable. In addition, the VD-model may be more rational because it considers both volumetric and deviatoric creep equations. However, it dose underestimate the creep deformation in real engineering applications. The model needs to be improved through introducing correction factors.

In this work, all the soft clays exhibit two creep phases, including decay creep and steady creep, without an accelerated phase of the creep. Some scholars have found that at higher shear stress levels, certain soft clays show accelerated creep (Jiang *et al*. 2014) and the predictions of the three models deviate from test data. It is widely assumed that the overstress theory is unable to express accelerated phase of the creep. In addition, creep behavior of soft clay differs from elastic-plastic deformation. There are shortcomings associated with the cam clay plasticity framework used in creep. Thus, the proposed model needs to be improved further by considering rate-dependent properties, non-associated flow and different flow rule.

The soft clays in this study are distributed in coastal areas of China and around the Yangtze River. The basic physical properties of these soft clays are as follows: water content ω > 60%, liquid limit ω_l = 60%-80%, plastic limit ω_p = 27%-30%. Based on the models' performance, it can be inferred that the models are suitable for soft clays with high water content and compressibility. A broad investigation involving more potential factors is needed. However, the proposed models currently focus on the effects of consolidation stress, shear stress level and stress ratio. It is essential to enhance the model's performance for different situations. Therefore, the models need to consider additional factors, such as consolidation ratio, shear rate, and so on. These researches would benefit the engineering practice.

6. Conclusions

In the work, two updated hyperbolic equations based on the volumetric creep and deviatoric creep are proposed, respectively. Subsequently, three creep constitutive models based on different creep behavior are developed and compared. The main conclusions include (1) The D-model shows the most accurate predictions with strong model stability. The V-model also predicts the creep deformation accurately. However, it exhibits high parametric sensitivity.

The VD-model shows the lowest parametric sensitivity, but its predicted values consistently fall below the test data. This discrepancy may lead to an underestimation of creep deformation in real engineering applications. Therefore, it is recommended that the D-model be prioritized in engineering practice. (2) The VD-model successfully captures the dilative behavior of the examined soils. The utilization of the Mises yield function in the flow surface, as adopted by the VD-model, seems more reasonable. This implies that the flow surface significantly influences the model's predictions. Hence, there is a pressing need to identify a more suitable flow surface function. (3) The models should incorporate additional factors, such as consolidation ratio, shear rate, water content, and so on. These areas deserve further investigation, and this research should serve as a guide for engineering practice, ultimately benefiting engineering applications.

Acknowledgments

The research described in this paper was financially supported by the Postgraduate Research & Practice Innovation Program of Jiangsu Province (No. KYCX22_0623), the scientific project from Huaneng company Headquarters (HNKJ20-H45), 111 Project (No. B13024) and the Open Sharing Fund for the Large-scale Instruments of Hohai University (GX202205B, GX202204B).

References

Acharya, M.P., Hendry, M.T. and Martin, C.D. (2018), "Creep behavior of intact and remold fibrous peat", *Acta Geotechnica*, **13**, 399-417. https://doi.org/10.1007/s11440-017-0545-1.

Bi, G., Ren, C., Xu, H.Z. and Jiang, D.Q. (2022), "Creep behavior of cohesive soils associated with different plasticity indexes", *Environ. Earth Sci.*, **81**, 151. https://doi.org/10.1007/s12665-022-10271-6.

Borja, R.I. and Kavazanjian, Jr, E. (1985), "A constitutive model for the stress-strain-time behavior for "wet" clays", *Géotechnique*, **35**(3), 183-198. https://doi.org/10.1680/geot.1985.35.3.283.

Borja, R.I. (1992), "Generalized creep and stress relaxation model for clays", *J. Geotech. Eng. (ASCE)*, **118**(11), 1765-1786. https://doi.org/10.1061/(ASCE)0733-9410(1992)118:11(1765).

Chen, B., Xu, Q. and Sun, D.A. (2014), "An elastoplastic model for structured clays", *Geomech. Eng*., 7(2), 213-231. https://doi.org/ 10.12989/gae.2014.7.2.213.

Chen, X.P., Huang, G.Y. and Liang, Z.S. (2003), "Study on soft properties of the pearl river delta", *Chinese J. Rock Mech. Eng.*, 1, 137-141. https://doi.org/1000-6915(2003)01-0137-05. (in Chinese).

Chen, Z.J., Feng, W.Q. and Yin, J.H. (2021), "A new simplified method for calculating short-term and long-term consolidation settlements of multi-layered soils considering creep limit", *Comput. Geotech*., **138**(2021), 104324. https://doi.org/10.1016/j.compgeo.2021.104324.

Dong, W.J. (2007), "Study on the laboratory test of rheological characteristic of soft clay and long-term strength", PH.D. Dissertation, Hohai University, Nanjing, Jiangsu, China.

Freitas, T., Potts, D.M. and Zdravkovic, L. (2011), "A time dependent constitutive model for soils with isotach viscosity", *Comput. Geotech*., **38**(6), 809-820. https://doi.org/10.1016/j.compgeo.2011.05.008.

Hessam, Y. and Mohammad, M.T. (2012), "Nonlinear consolidation of soft clays subjected to cyclic loading-part II: verification and application", *Geomech. Eng*., **4**(4), 243-249. https://doi.org/ 10.12989/gae.2012.4.4.243.

Hsieh, H.S., Kavazanjian, E.J. and Borja, R.I. (1990), "Double-

yield-surface cam-clay plasticity model. i: theory", *J. Geotech. Eng*., **116**(9). https://doi.org/10.1061/(ASCE)0733-9410(1990)116:9(1381).

Hu, J.L. (2013), "The study of creep characteristics for soft clay and its application on calculation of long-term subgrade settlement", PH.D. Dissertation, Hohai University, Nanjing, Jiangsu, China.

Jiang, Y.Q. and Mu, X.Y. (1984), *Plastic Mechanics Foundation*, China Machine Press, Beijing, China.

Kavvadas, M. and Kalos, A. (2019), "A time-dependent plasticity model for structured soils (TMS) simulating drained tertiary creep", *Comput. Geotech*., **109**, 130-143.

Li, C. (2019), "Study on the loading and deformation of tunnel segments in soft clay with consideration for the soil mass rheological characteristics", *Geotech. Geol. Eng*., **37**(2), 1-10. https://doi.org/10.1007/s10706-018-0637-1.

Liu, W.Z., Shi, Z.G., Zhang, J.H. and Zhang, D.W. (2019), "One-dimensional nonlinear consolidation behavior of structured soft clay under time-dependent loading", *Geomech. Eng*., **18**(3), 299-313. https://doi.org/ 10.12989/gae.2019.18.3.299.

Liu, Y.F. (2020), "Experimental study on consolidation rheological properties of Cangzhou coastal", PH.D. Dissertation, North China University of Water Resources and Electric Power. Zhengzhou, Henan, China.

Liu, Y.H. (2008), "Study on engineering property and application of constitutive model for Ningbo soft clay", Ph.D. Dissertation, Zhe Jiang University, Hangzhou, Zhejiang, China.

Long, Z.L., Cheng, Y.Z., Yang, G.Y., Dong, Y. and Xu, Y.L. (2021), "Study on triaxial creep test and constitutive model of compacted red clay", *Int. J. Civil Eng*., **19**, 517-531. https://doi.org/10.1007/s40999-020-00572-x.

Mesri, G., Eehres-Cordero, E. and Shields, D.R. (1981), "Shear stress-strain-time behaviour of clays", *Géotechnique*, **31**(4), 537-552. https://doi.org/10.1680/geot.1981.31.4.537.

Morsy, M.M., Chan, D.H. and Morgenstern, N.R. (1995), "An effective stress model for creep of clay", *Can. Geotech. J*., **32**(5), 819-834. https://doi.org/10.1139/t95-079

Oliveira, P., Santos, S.L., Correia, A. and Lemos, L. (2019), "Numerical prediction of the creep behaviour of an embankment built on soft soils subjected to preloading", *Comput. Geotech*., **114**, 103140. https://doi.org/10.1016/j.compgeo.2019.103140.

Perzyna, P. (1966), "Fundamental problems in viscoplasticity", *Adv. Appl. Mech*., **9**(2), 243-377. https://doi.org/10.1016/S0065-2156(08)70009-7.

Qiao, Y., Ferrari, A., Laloui, L. and Ding, W. (2016), "Nonstationary flow surface theory for modeling the viscoplastic behaviors of soils", *Comput. Geotech*., **76**, 105-119. https://doi.org/10.1016/j.compgeo.2016.02.015.

Ramadhika, F., Kristyanto, T., Indra, T.L. and Syahputra, R. (2018), "The responsibility of high activity clay mineral toward landslide occurrence in volcanic sediment area, Cianjur", *Proceedings of the 3rd international symposium on current progress in mathematics and sciences 2017 (iscpms2017)*.

Rezania, M., Taiebat, M. and Poletti, E. (2016), "A viscoplastic SANICLAY model for natural soft soils", *Comput. Geotech*., **73**, 128-141. https://doi.org/10.1016/j.compgeo.2015.11.023.

Roscoe, K.H. and Burland, J.B. (1968), *Engineering Plasticity*, Cambridge University Press, Cambridge, England.

Singh, A. and Mitchell, J.K. (1968), "General stress-strain-time function for soils", *J. Soil Mech. Found. Division*, **94**(1), 21-46. https://doi.org/10.1061/JSFEAQ. 0001084.

Taylor, D.W. (1948), *Fundamentals of Soil Mechanics*, Wiley and Sons, New York, America.

Thu, M.L., Behzad, F., Mahdi, D. and Hadi, K. (2015), "Analyzing consolidation data to obtain elastic viscoplastic parameters of clay", *Geomech. Eng*., **8**(4), 559-594. https://doi.org/ 10.12989/gae.2015.8.4.559.

Venda Oliveira, P.J., Santos, S.L., Correia, A.A.S. and Lemos, L.J.L. (2019), "Numerical prediction of the creep behaviour of an embankment built on soft soils subjected to preloading", *Comput. Geotech*., **114**, 103140.

von Mises, R. (1913), "Mechanik der festen Körper im plastisch deformablen Zustand. Nachrichten von der Königlichen Gesellschaft der Wissenschaften zu Göettingen", *Mathematisch-physikalische Klasse*, (1) 582-592.

Yao, Y.P., Kong, L.M. and Zhou, A.N. (2015), "Time-dependent unified hardening model: three-dimensional elasto-visco-plastic consti- tutive model for clays", *J. Eng. Mech*., **141**(6). https://doi.org/10.1061/(ASCE)EM.1943-7889.0000885.

Yin, J.H. and Graham, J. (1989), "Viscous-elastic-plastic modelling of one dimensional time-dependent behavior of clays", *Can. Geotech. J*., **26**, 199-209. https://doi.org/10.1139/t89-029.

Yin, J.H. and Graham, J. (1994), "Equivalent times and one-dimensional elastic visco-piastic modelling of time-dependent stress-strain behavior of clays", *Can. Geotech. J*., **31**, 42-52. https://doi.org/10.1016/0148-9062(94)90219-4.

Yin, J.H. (1999), "Equivalent time and elastic visco-plastic models for geomaterials", *Chinese J. Rock Mech. Eng*., **18**(2), 124-128.

Yin, Q., Zhao, Y., Gong, W.M., Dai, G.L., Zhu, M.X., Zhu, W.B. and Xu, F. (2023), "A fractal order creep-damage constitutive model of silty clay", *Acta Geotechnica*, **18**, 3997-4016. https://doi.org/10.1007/s11440-023-01815-6.

Zhao, T.B., Zhang, Y.B., Zhang, Q.Q. and Tan, Y.L. (2018), "Analysis on the creep response of bolted rock using bolted burgers model", *Geomech. Eng*., **14**(2), 141-149. https://doi.org/10.12989/gae.2018.14.2.141.

Zhu, H.H., Chen, X.P., Cheng, X.J. and Zhang, B. (2006), "Study on creep characteristics and model of soft soil considering drainage condition", *Rock Soil Mech.*, **27**(5), 694-698. https://doi.org/10.16285/j.rsm.2006.05.003.

Zhu, Q.Y., Jin, Y.F. and Yin, Z.Y. (2019), "Modeling of embankment beneath marine deposited soft sensitive clays considering straightforward creep degradation", *Mar. Georesour. Geotec*., (5), 1-17. https://doi.org/10.1080/1064119X.2019.1603254.

Zhu, Q.Y., Yin, Z.Y., Xu, C.J., Yin, J.H. and Xia, X.H. (2015), "Uniqueness of rate-dependency, creep and stress relaxation behaviors for soft clays", *J. Central South Univ*., **22**(1), 296-302. https://doi.org/10.1007/s11771-015-2521-y.

GC

Appendix A

Under triaxial stress state, there is the following relationship between stresses

$$\begin{cases} \sigma_2=\sigma_3 \\ p=\dfrac{\sigma_1+\sigma_2+\sigma_3}{3}=\dfrac{\sigma_1+2\sigma_3}{3} \\ q=\sigma_1-\sigma_3 \end{cases} \tag{22}$$

Similar to the MCC model, the elastic-plastic strain components are shown by Eq. (23) and Eq. (24).

$$d\varepsilon_{ij}^{e}=\frac{1+\mu}{3(1-2\mu)}\frac{\kappa}{1+e_0}pd\sigma_{ij}-\frac{\mu}{(1-2\mu)}\frac{\kappa}{1+e_0}dp\delta_{ij} \tag{23}$$

$$d\varepsilon_{ij}^{e}=\frac{1+\mu}{3(1-2\mu)}\frac{\kappa}{1+e_0}pd\sigma_{ij}-\frac{\mu}{(1-2\mu)}\frac{\kappa}{1+e_0}dp\delta_{ij} \tag{24}$$

where E is module of elasticity. κ is the slope of the reloading curve after the rebound of the isotropic consolidation test in e-ln$p$ plane. μ is Poisson's ratio. e_0 is the initial void ratio. δ_{ij} represents the stress value under general stress state. δ_{ij} is a Kronecker symbol, when $i=j$, $\delta_{ij}=1$, otherwise 0. λ is the slope of the loading curve of the isotropic consolidation test in e-ln$p$ plane.

$$d\varepsilon_{ij}^{e}=\frac{1+\mu}{3(1-2\mu)}\frac{\kappa}{1+e_0}pd\sigma_{ij}-\frac{\mu}{(1-2\mu)}\frac{\kappa}{1+e_0}dp\delta_{ij} \tag{24}$$

Appendix B. V-model

Substituting Eqs. (17) and (23)-(24) into Eq. (10), the constitutive model (V-model) is expressed by

$$\begin{aligned} &\{d\varepsilon_{ij}\}=\{d\varepsilon_{ij}^{e}\}+\{d\varepsilon_{ij}^{p}\}+\{d\varepsilon_{ij}^{c}\} \\ &=\frac{1+\mu}{3(1-2\mu)}\frac{\kappa}{1+e_0}pd\sigma_{ij}-\frac{\mu}{(1-2\mu)}\frac{\kappa}{1+e_0}dp\delta_{ij} \\ &+\frac{\lambda-\kappa}{1+e_0}\left\{\frac{M^2p^2-q^2}{M^2p^2+q^2}\frac{\delta_{ij}}{3p}+\frac{3(\sigma_{ij}-p\delta_{ij})}{M^2p^2+q^2}\right\}\left(dp+\frac{2pq}{M^2p^2-q^2}dq\right) \\ &+\frac{\left[\dfrac{\delta_{ij}}{3}+\dfrac{3p(\sigma_{ij}-p\delta_{ij})}{M^2p^2-q^2}\right]\left[1-\varepsilon_v^{c}k_{v2}\left(\dfrac{q}{p}\right)^{-n_{v2}}\right]^2}{\left[k_{v1}\left(\dfrac{q}{p_a}\right)^{-n_{v1}}t_0\right]}dt \end{aligned} \tag{25}$$

Appendix C. D-model

Substituting Eqs. (19) and (23)-(24) into Eq. (10), the constitutive model (D-model) is expressed by

$$\begin{aligned} &\{d\varepsilon_{ij}\}=\{d\varepsilon_{ij}^{e}\}+\{d\varepsilon_{ij}^{p}\}+\{d\varepsilon_{ij}^{c}\} \\ &\frac{1+\mu}{3(1-2\mu)}\frac{\kappa}{1+e_0}pd\sigma_{ij}-\frac{\mu}{(1-2\mu)}\frac{\kappa}{1+e_0}dp\delta_{ij} \\ &+\frac{\lambda-\kappa}{1+e_0}\left\{\frac{M^2p^2-q^2}{M^2p^2+q^2}\frac{\delta_{ij}}{3p}+\frac{3(\sigma_{ij}-p\delta_{ij})}{M^2p^2+q^2}\right\}\left(dp+\frac{2pq}{M^2p^2-q^2}dq\right) \\ &+\left[\frac{M^2p^2-q^2}{M^2p^2+q^2}\frac{\delta_{ij}}{3p}+\frac{3(\sigma_{ij}-p\delta_{ij})}{2q}\right]\frac{\left[1-\varepsilon_s^{c}k_{s2}\left(\dfrac{q}{p}\right)^{-n_{s2}}\right]^2}{\left[k_{s1}\left(\dfrac{q}{p_a}\right)^{-n_{s1}}t_0\right]}dt \end{aligned} \tag{26}$$

Appendix D. VD-model

Substituting Eqs. (21) and (23)-(24) into Eq. (10), the constitutive model (VD-model) is expressed by

$$\begin{aligned} &\{d\varepsilon_{ij}\}=\{d\varepsilon_{ij}^{e}\}+\{d\varepsilon_{ij}^{p}\}+\{d\varepsilon_{ij}^{c}\} \\ &=\frac{1+\mu}{3(1-2\mu)}\frac{\kappa}{1+e_0}pd\sigma_{ij}-\frac{\mu}{(1-2\mu)}\frac{\kappa}{1+e_0}dp\delta_{ij} \\ &+\frac{\lambda-\kappa}{1+e_0}\left\{\frac{M^2p^2-q^2}{M^2p^2+q^2}\frac{\delta_{ij}}{3p}+\frac{3(\sigma_{ij}-p\delta_{ij})}{M^2p^2+q^2}\right\}\left(dp+\frac{2pq}{M^2p^2-q^2}dq\right) \\ &+\frac{I}{3}\frac{\left[1-\varepsilon_v^{c}k_{v2}(q/p)^{-n_{v2}}\right]^2}{\left[k_{v1}(q/p_a)^{-n_{v1}}t_0\right]}dt+\frac{\left[1-\varepsilon_s^{c}k_{s2}(q/p)^{-n_{s2}}\right]^2}{\left[k_{s1}(q/p_a)^{-n_{s1}}t_0\right]}\frac{\{s_{ij}\}}{q}dt \end{aligned} \tag{27}$$

Appendix E

The major principal strain and minor principal strain of creep strain of the three models are shown as follows to depict Figs. 8-12.

The major principal strain and minor principal strain of creep for V-model

$$\{d\varepsilon_1^{c}\}=\left[\frac{1}{3}+\frac{3p(\sigma_1-p)}{M^2p^2-q^2}\right]\frac{\left[1-\varepsilon_v^{c}k_{v2}(q/p)^{-n_{v2}}\right]^2}{\left[k_{v1}(q/p_a)^{-n_{v1}}t_0\right]}dt \tag{28}$$

$$\{d\varepsilon_3^{c}\}=\left[\frac{1}{3}+\frac{3p(\sigma_3-p)}{M^2p^2-q^2}\right]\frac{\left[1-\varepsilon_v^{c}k_{v2}(q/p)^{-n_{v2}}\right]^2}{\left[k_{v1}(q/p_a)^{-n_{v1}}t_0\right]}dt \tag{29}$$

The major principal strain and minor principal strain of creep for D-model

$$\{d\varepsilon_1^{c}\}=\left[\frac{M^2p^2-q^2}{2q}\frac{1}{3p}+\frac{3(\sigma_1-p)}{2q}\right]\frac{\left[1-\varepsilon_s^{c}k_{s2}(q/p)^{-n_{s2}}\right]^2}{\left[k_{s1}(q/p_a)^{-n_{s1}}t_0\right]}dt \tag{30}$$

$$\{d\varepsilon_3^{c}\}=\left[\frac{M^2p^2-q^2}{2q}\frac{1}{3p}+\frac{3(\sigma_3-p)}{2q}\right]\frac{\left[1-\varepsilon_s^{c}k_{s2}(q/p)^{-n_{s2}}\right]^2}{\left[k_{s1}(q/p_a)^{-n_{s1}}t_0\right]}dt \tag{31}$$

The major principal strain and minor principal strain of creep for VD-model

$$\{d\varepsilon_1^{c}\}=\frac{I}{3}\frac{\left[1-\varepsilon_v^{c}k_{v2}(q/p)^{-n_{v2}}\right]^2}{\left[k_{v1}(q/p_a)^{-n_{v1}}t_0\right]}dt+\frac{\left[1-\varepsilon_s^{c}k_{s2}(q/p)^{-n_{s2}}\right]^2}{\left[k_{s1}(q/p_a)^{-n_{s1}}t_0\right]}\frac{\sigma_1-p}{q}dt \tag{32}$$

$$\{d\varepsilon_3^{c}\}=\frac{I}{3}\frac{\left[1-\varepsilon_v^{c}k_{v2}(q/p)^{-n_{v2}}\right]^2}{\left[k_{v1}(q/p_a)^{-n_{v1}}t_0\right]}dt+\frac{\left[1-\varepsilon_s^{c}k_{s2}(q/p)^{-n_{s2}}\right]^2}{\left[k_{s1}(q/p_a)^{-n_{s1}}t_0\right]}\frac{\sigma_3-p}{q}dt \tag{33}$$